4th Micro and Nano Flows Conference
UCL, London, UK, 7-10 September 2014

Kinetic calculation of rarefied gaseous flows in long tapered rectangular microchannels

Lajos SZALMAS [1,*]

* Corresponding author: Tel.: ++49 (0)421 218 63495; Email: lszalmas@gmail.com
1 Center for Environmental Research and Sustainable Technology (UFT),
University of Bremen, Germany

Abstract Gaseous flows in microsystems have attracted considerable attention in fluid dynamic communities over the last few years. When the size of the device is in the range of microns, the molecular mean free path becomes comparable with the device size, and the details of the molecular interactions need to be taken into account. The proper description of such microflows requires the consideration of the velocity distribution function of the molecules and kinetic equations. The scope of the present paper is to discuss the determination of the behavior of pressure driven rarefied gas flows in microchannels at the kinetic level. As a new application of the methodology, preliminary results are presented for pressure driven flows of single gases through long rectangular tapered microchannels, which have constant widths but varying depths along the axis of the channel. The kinetic calculation is based on the solution of the linearized Bhatnagar-Gross-Krook (BGK) equation and refers to the determination of the mass flow rate through the channel and the axial distribution of the pressure. The BGK equation is solved by the discrete velocity method. It is shown that the mass flow rate exhibits the diodicity effect, which means that the flow rate depends on the orientation of the channel. If the gas flows from the larger cross section towards the smaller one, the flow rate is larger than in the opposite situation. The pressure profile strongly varies near the small cross section, and it has a quite different character than in the case of channels with uniform cross sections. The tapered microchannel might be useful for separating the different gaseous components in engineering applications.

Keywords: Rarefied Gas Flows, Tapered Microchannels, Kinetic Calculation, BGK Equation

1. Introduction

Over the last few years, flows of rarefied gases in microsystems have attracted significant scientific interest, which is well justified by the appearance of gaseous micro and nanoflows [1,2]. The Knudsen number, the ratio of the molecular mean free path and the characteristic size of the flow, is the relevant quantity to classify the flows of rarefied gases. In microsystems, the Knudsen number can be in a wide range from the hydrodynamic and slip regimes to the transition region. When the mean free path is comparable with the characteristic length, the proper description should be based on the kinetic level, i.e. the velocity distribution function and kinetic equations [3].

Although considerable effort has been made to solve kinetic equations for rarefied gases, the numerical modeling of these flows is still challenging. In micro and nanoflows, typically the flow is through micro or nanochannels. Important geometrical parameters of the channel consist of its cross section shape, with the relevant dimensions, and the length of the channel. There are major differences whether the length is comparable with the characteristic cross sectional dimension, or the length is much larger than this dimension. In the former case, the channel is considered short, the speed of the gas can be comparable with its average molecular speed and the description requires non-linear equations. However, in typical microfluidic applications, the channel is long. In this situation, the speed of the gas is small compared to the mean molecular speed and the flow can be described by linear kinetic equations. Another important feature of long channels is that the flow is only in the axial direction and the effects of the channel inlet

and outlet can be neglected.

Significant work has been devoted to model single gas flows through long channels on the basis of linearized kinetic equations. For such flows, the modeling of the flow consists of two steps. First, the local flow problem in the cross section sheet, where the gas is subject to the local driving forces, is solved. Since the flow is linear, an arbitrary flow can be obtained by the composition of basic flows driven by unity driving forces. The local flow problem depends on the cross section sheet and the local Knudsen number or the rarefaction parameter, which is proportional with the inverse of the former and typically used in rarefied gas dynamics to describe the flow. After the local flow problem is solved, the global flow can be obtained in a second step by the consideration of the conservation of the mass of the gas.

The flow can be described by linearized kinetic models, such as the Bhatnagar-Gross-Krook (BGK) or Shakov models, or the original Boltzmann equation. The usefulness of kinetic models is that they have simpler mathematical structures than the original Boltzmann equation. The simplicity results in an easier mathematical solution. Kinetic equations are integro-differential. Their analytical solution exists only in special cases, and typically, they need to be solved numerically.

The numerical methods for the solution of kinetic equations can be either deterministic or probabilistic. Among the deterministic approaches, the discrete velocity method is the most common one. In this case, the molecular velocity, spatial (and temporal) spaces are discretized. The differential operators and the integrals are approximated by finite differences and quadratures. The resulting discrete equations are then solved computationally. For istothermal pressure driven flows, the BGK kinetic equation has been solved by the discrete velocity method for single gas flows through uniform channels with rectangular [4], circular [5,6], elliptical [7], triangular [8,9] or trapezoidal [10] cross sections.

Among the probabilistic approaches, the Direct Simulation Monte Carlo (DSMC) is the most popular one [11]. In this situation, the gas is modeled by the collection of a large amount of test particles, which mimic the real motion of molecules in the considered geometry. The kinetic equation is solved by the splitting approach. In the streaming step, the movement of the molecules is simulated, while in the collision step, the molecular interactions are modeled in a probabilistic manner. The macroscopic moments are obtained as averages. The DSMC is especially well-suited for high-speed flows, when the signal to noise ratio is relatively large. For low-speed flows, which are typical in microfluidic applications, the DSMC is not suitable since the simulation requires very long time. For low-speed flows, the recently developed low-variance or variance-reduced DSMC can be used [12,13,14].

Previous works have mainly referred to flows through a uniform single channel. However, in applications, other, more complicated flow configurations can exist. For example, the channels are often connected into a network. In this case, the challenge is to determine the flow by considering all initially unknown boundary conditions at the inlet and the outlet of the channels. The problem has recently been solved for the general case of gaseous mixtures in the whole range of the rarefaction [15]. Another interesting situation is when the channel is still long, but the cross section is not uniform. Such a flow configuration has not been investigated in the literature at the kinetic level with full complexity. When the channel has rectangular cross section shape, but its particular dimensions slowly vary along the axis, the channel is referred as tapered.

The scope of the paper is to discuss the kinetic calculation of isothermal single gas flows in long rectangular channels with varying cross sections. The theoretical and numerical treatments used in the associated kinetic calculation are presented. Preliminary results in terms of the flow rates and typical profiles of the pressure and rarefaction parameter along the axis of the channel are delivered and commented on.

2. Statement of the problem

Isothermal flow of a rarefied gas in a long channel is considered. The channel axis lies along the z' coordinate direction, while its cross section is in the (x',y') coordinate sheet. The length of the channel is denoted by L. The channel has rectangular cross section. It is assumed that the width of channel, W, is constant, but its height is varying along the axis $H=H(z')$. The relative variance of the height is much smaller than unity

$$\frac{dH}{dz'} \ll 1. \qquad (1)$$

The flow is characterized by the local rarefaction parameter

$$\delta = \frac{Pl}{\mu v_0}, \qquad (2)$$

where P is the pressure, μ is the viscosity, $v_0=\sqrt{2k_B T/m}$ is the characteristic speed of the molecules and $l=H$ if $H \le W$ and $l=W$ otherwise. As it can be seen, l is defined as the smallest side of the rectangular cross section and plays the role of the relevant local spatial length scale. In the definition of the characteristic speed, k_B,T,m are the Boltzmann constant, the temperature and the molecular mass of the gas. The Knudsen number is also introduced by $Kn=\sqrt{\pi}/(2\delta)$.

The pressure and the rarefaction parameter at the inlet (A) and the outlet (B) are denoted by P_A,P_B and δ_A,δ_B. It is supposed that $P_A>P_B$; hence, the flow is from the inlet towards the outlet.

The main interest of the present work is in the mass flow rate defined by

$$\dot{M} = \int \rho u'_z dA, \qquad (3)$$

where ρ,u'_z are the local mass density and the axial velocity of the gas, and A denotes the cross section of the channel. The goal is to determine the flow rate and the axial distributions of the pressure and the rarefaction parameter for specific flow configurations.

3. Method of solution

Since the channel is long and the assumption of Eq. (1) is hold, the solution of the problem can be divided into two stages. Locally, the flow can be considered along the axial direction and the transverse velocities can be neglected. It is driven by the local axial pressure gradient. This local flow problem is solved by using kinetic description. After the local flow is known, the global flow behavior can be deduced by the consideration of the conservation of the mass along the axial direction.

The present work includes the special case when the height of the channel is constant. Hence, previous findings are reviewed.

3.1. Kinetic description

At the kinetic level, the flow is presented in terms of the velocity distribution function of the molecules $f(v,x',y',z')$, where v denotes the molecular velocity. The distribution function obeys a particular kinetic equation. In the present work, the BGK equation is considered, which provides physically accurate results for isothermal flows.

Dimensionless coordinates and molecular velocity are introduced according to $x=x'/l$, $y=y'/l$, $z=z'/l$ and $c=v/v_0$. The distribution function is linearized such that

$$f(c,x,y,z) = f_0(c,z)\left[1+h(c,x,y)\right], \qquad (4)$$

where $h(c,x,y)$ is the perturbation function and

$$f_0(c,z) = n(z)\pi^{-3/2} v_0^{-3} \exp\left(-c^2\right) \qquad (5)$$

is the equilibrium distribution function.

The perturbation function obeys the linearized BGK equation

$$c_x \frac{\partial h}{\partial x} + c_y \frac{\partial h}{\partial y} = -\delta h + \delta 2c_z u_z - X_p c_z, \qquad (6)$$

where

$$u_z = \pi^{-3/2} \int h c_z e^{-c^2} dc \qquad (7)$$

is the dimensionless velocity and

$$X_p = \frac{dn}{dz}\frac{1}{n} \tag{8}$$

is the local density gradient, which drives the flow.

The kinetic equation is considered on the cross section of the channel. In order to define the problem well, the boundary condition for the incoming velocity directions at the perimeter of the cross section is to be defined. In the present work, the diffuse reflection boundary condition is applied. In this situation, the outgoing molecules accommodate at the channel wall and are reflected to the gas phase in a diffuse manner. The diffuse boundary condition for the perturbation function is written by

$$h\left(c_i, x_p, y_p\right) = 0, \tag{9}$$

where the subscripts *i* and *p* refer to the incoming velocity directions and the perimeter, respectively.

After solving the kinetic problem, the velocity profile is known on the cross section sheet. Since the problem is linear, the velocity profile can be obtained as a linear function of the local dimensionless density gradient. The dimensionless flow rate

$$G(\delta, a) = -\frac{2}{AX_p}\int u_z dA \tag{10}$$

has a cardinal importance. It provides twice the absolute value of the spatial average of the velocity on the cross section sheet for a unity driving term. It is emphasized that *G* depends on the local rarefaction parameter and the aspect ratio of the channel defined by $a = H/W$ if $H \le W$ and $a = W/H$ otherwise. The dimensionless flow rate is used to determine the flow rate for a global pressure driven flow.

3.2. Local flow problem

The kinetic equation is to be solved numerically. For this reason, it is worth simplifying the overall problem by introducing the new distribution function

$$Y\left(c_x, c_y, x, y\right) = \pi^{-1/2}\int h\, c_z e^{-c_z^2} dc_z . \tag{11}$$

In terms of this function, the kinetic equations reads such that

$$c_x\frac{\partial Y}{\partial x} + c_y\frac{\partial Y}{\partial y} = -\delta Y + \delta u_z - \frac{X_p}{2}, \tag{12}$$

where

$$u_z = \pi^{-1}\iint h\, e^{-c_x^2 - c_y^2} dc_x dc_y . \tag{13}$$

The boundary condition for the new distribution function is written by

$$Y\left(c_{ix}, c_{iy}, x_p, y_p\right) = 0. \tag{14}$$

As it was mentioned in the introduction, kinetic equations are typically solved by either deterministic or probabilistic approaches. In the present work, it is solved by the discrete velocity method.

In the standard discrete velocity method, the spatial and velocity spaces are discretized. Here, the spatial coordinates are discretized into *MxM* nodes, while the velocity space is represented by a quadrature. The velocity magnitude is given by an *N*-point Gauss-Legendre quadrature and the $\pi/2$ angle interval is divided into *K* nodes. The spatial derivatives of Eq. (12) are approximated by finite-differences, while the integral in Eq. (13) is calculated by the quadrature. The kinetic equation is solved iteratively. By assuming an initial state for the velocity field, Eq. (12) is solved for the distribution function. Then, the velocity is calculated from Eq. (13) and inserted back to the kinetic equation. The overall procedure is repeated until a converged result is not reached.

The above mentioned standard iteration is slow near the hydrodynamic limit. In order to reduce the required number of iterations, the accelerated discrete velocity method can be used [9,6]. This method has been developed for both single gases and gaseous mixtures. Additional moment equations are derived on the basis of the kinetic equation. These additional equations are solved parallel with the original kinetic one in a coupled iteration. Such an approach significantly accelerates the solution near the hydrodynamic limit. Hence,

by using the accelerated method, results for the local flow problem can be obtained in a convenient manner in the whole range of gaseous rarefaction.

In the present work, the following moment equation derived from Eq. (12) is used

$$\Delta u_z = -2\partial_x^2 M_x - 2\partial_y^2 M_y - 4\partial_x \partial_y M_{xy} - \delta X_p, \quad (15)$$

where

$$M_a = \pi^{-1} \iint Y \left(c_a^2 - \frac{1}{2} \right) e^{-c_x^2 - c_y^2} dc_x dc_y, \quad (16)$$

$$M_{xy} = \pi^{-1} \iint Y c_x c_y e^{-c_x^2 - c_y^2} dc_x dc_y \quad (17)$$

with $a = [x,y]$.

In the accelerated iteration, after Eq. (12) is solved in an iteration stage, the higher moments are calculated, and the velocity is deduced by solving the moment equation. Then, this velocity is inserted into Eq. (12), and the overall iteration is repeated until a desirable convergence is not reached. The moment equation is solved by the finite difference method on the same grid as used for the kinetic equation. The velocity at the boundaries is not accelerated, but used as the boundary condition for the moment equation.

In the discrete velocity solution, the following parameters have been applied: M=[151, 301] for $\delta \le 10$ and otherwise, N=16 and K=[100,300] for $\delta \le 2$ and otherwise. The dimensionless flow rate is calculated with numerical accuracy better than 0.05% for a wide range of the rarefaction and numerous values of the aspect ratio. In the ranges of $\delta < 2$ and $2 \le \delta \le 230$, the non-accelerated and accelerated methods have been used. For $\delta > 230$ the slip flow formula in Ref. [4] is used to deduce G.

3.3. Global behavior

The overall pressure driven flow in the channel can be determined by the conservation of mass. The mass flow rate can be written by

$$\dot{M} = -G(\delta, a) \frac{HWl}{v_0} \frac{dP}{dz'}. \quad (18)$$

This differential equation is equipped with the boundary conditions for P and solved to obtain the pressure distribution and the mass flow rate. It is noted that in Eq. (18), G, H and l are local quantities to be known at every points along the axis of the channel. G is determined on the basis of the precomputed database mentioned in the previous section.

The solution of Eq. (18) is carried out by discretizing the spatial coordinate $z'_i = (i-1)\Delta z'$, where $1 \le i \le I$ and $\Delta z' = L/(I-1)$. The equation is solved by the following two step scheme

$$P'_i = P_{i-1} - \frac{\dot{M} v_0 \Delta z'}{2G(\delta_{i-1}, a'_i) H'_i W l'_i}, \quad (19)$$

$$P_i = P_{i-1} - \frac{\dot{M} v_0 \Delta z'}{G(\delta'_i, a'_i) H'_i W l'_i}, \quad (20)$$

where the subscripts i and i-1 denote the quantities at z'_i, z'_{i-1}, respectively, and the superscript ' stands for the intermediate value at $(z'_i + z'_{i+1})/2$. The mass flow rate is chosen in such a way that after the integration of Eqs. (19)-(20), the boundary conditions are fulfilled. In the actual calculation, the value I=10000 has been applied.

4. Results

Pressure driven flow is calculated through a specific tapered channel with a linearly varying height. The small height is denoted by H_S, the large height is H_L=100H_S and the width is W=500H_S. If the large height is at the inlet, the flow direction is referred as nozle, and it is diffusor in the opposite situation. The length of the channel does not play role in the calculation. The dimensionless mass flow rate is defined by

$$J = \frac{v_0 L}{P_B^N (\Pi^N + 1) H_S W H_L} \dot{M} \quad (21)$$

Table 1: Dimensionless flow rates versus outlet rarefaction parameter (left) or pressure ratio (right).

δ_B^N	Kn_m^N	J^N	Kn_m^D	J^D	D		Π	Kn_m^N	J^N	Kn_m^D	J^D	D
1.00E-2	4.44E+1	1.612	5.98E+0	1.550	1.040		2	1.11	0.569	5.65E-1	0.539	1.057
2.00E-2	2.22E+1	1.484	2.99E+0	1.390	1.067		3	1.11	0.892	3.80E-1	0.816	1.092
4.00E-2	1.11E+1	1.398	1.50E+0	1.270	1.100		4	1.11	1.115	2.88E-1	0.997	1.118
7.00E-2	6.34E+0	1.369	8.55E-1	1.220	1.123		5	1.11	1.288	2.33E-1	1.133	1.137
1.00E-1	4.44E+0	1.374	5.98E-1	1.205	1.140		6	1.11	1.432	1.96E-1	1.245	1.150
2.00E-1	2.22E+0	1.454	2.99E-1	1.250	1.162		7	1.11	1.558	1.69E-1	1.341	1.162
4.00E-1	1.11E+0	1.672	1.50E-1	1.430	1.169		8	1.11	1.672	1.50E-1	1.430	1.169
7.00E-1	6.34E-1	2.017	8.55E-2	1.744	1.156		9	1.11	1.776	1.34E-1	1.511	1.175
1.00E+0	4.44E-1	2.363	5.98E-2	2.071	1.141		10	1.11	1.874	1.22E-1	1.589	1.180
2.00E+0	2.22E-1	3.517	2.99E-2	3.196	1.100		11	1.11	1.968	1.12E-1	1.664	1.182
4.00E+0	1.11E-1	5.818	1.50E-2	5.483	1.061		12	1.11	2.057	1.03E-1	1.737	1.184
7.00E+0	6.34E-2	9.271	8.55E-3	8.931	1.038		13	1.11	2.143	9.63E-2	1.809	1.185
1.00E+1	4.44E-2	12.727	5.98E-3	12.384	1.028		14	1.11	2.227	9.02E-2	1.880	1.185

Table 2: Flow rates versus aspect ratio.

H_L/H_S	J^N	J^D	D
2	2.663E-2	2.543E-2	1.047
4	5.739E-2	5.233E-2	1.097
8	1.223E-1	1.078E-1	1.135
16	2.556E-1	2.211E-1	1.156
32	5.246E-1	4.502E-1	1.165

where $\Pi^N = P_A^N / P_B^N$ is the pressure ratio; in addition, P_A^N, P_B^N are the inlet and outlet pressures for the nozle case. The left side of Table 1 (first six columns) presents the dimensionless flow rates for both nozle (N) and diffusor (D) directions at $\Pi = 8$ versus outlet rarefaction parameter of the nozle case δ_B^N. The diffusor case is simulated with the same inlet and outlet pressures as used for the nozle direction. However, the results are classified by the outlet nozle rarefaction parameter. The average Knudsen number Kn^m is also shown in the table. A wide range of rarefaction is covered. It can be seen that both nozle and diffusor dimensionless flow rates exhibit the Knudsen minimum. An important finding is that the flow rate for the nozle case is always larger than the corresponding value for the diffusor direction. The diodicity defined by $D = J^N / J^D$ is shown in the sixth column of the table. The diodicity has a maximum in the transition region around, while it tends to zero in the hydrodynamic and free molecular limits. The right side of Table 1 (last six columns) shows the flow rates at this outlet rarefaction versus the pressure ratio. As it can be seen both flow rates and diodicity increase with increasing pressure ratio. Table 2 shows the flow rates and the diodicity for $\delta_B^N = 0.4$ and $\Pi = 8$ versus the ratio H_L/H_S. It is clearly seen that the diodicity is increasing with increasing H_L/H_S. Hence, the diodicity is larger for channels which are more tapered.

Figure 1 shows the axial distribution of the pressure and the rarefaction parameter for both directions at $\delta_B^N = 0.4$ and various values of the pressure ratio. P_0 is the outlet pressure for the nozle case. The pressure monotonically decreases along the axis in both cases. However, it exhibits a sharp change near the outlet and the inlet for the nozle and diffusor directions, respectively. The reason of this behavior is the monotonically varying cross section. The pressure profile is sharp near the small height. The rarefaction parameter behaves differently in the two directions. For the nozle and diffusor cases, it decreases and increases along the axis, respectively. In the diffusor direction, the increasing cross section along the axis overcomes the effect of the decreasing pressure, resulting into the unusual increasing rarefaction parameter. Such behavior is not observed for a channel with uniform cross section.

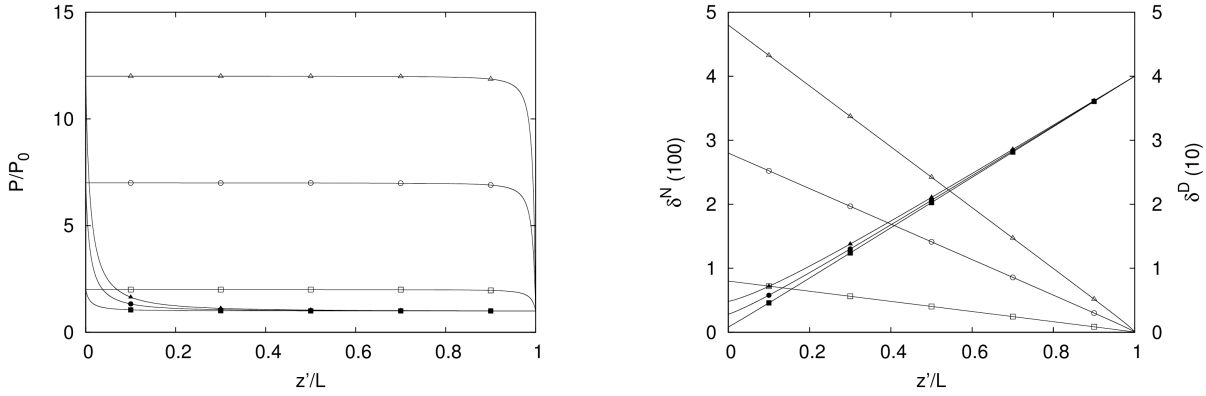

Figure 1: Axial distribution of pressure (left) and rarefaction parameters (right) for $\delta_B^N = 0.4$ *. Squares, circles and triangles stand for pressure ratio* [2, 7, 12]*, while empty and filled symbols represent results for the nozle (N) and diffusor (D) directions, respectively.*

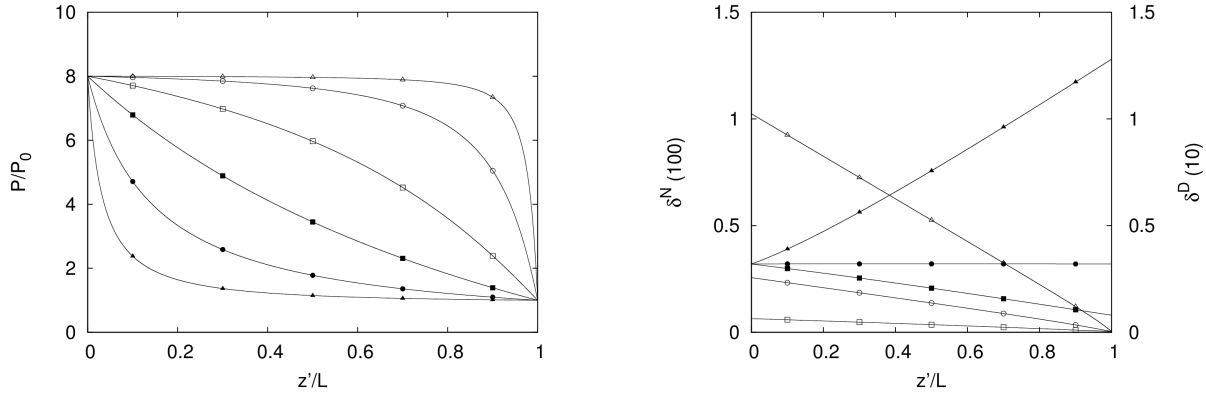

Figure 2: Axial distribution of pressure (left) and rarefaction parameter (right) for $\delta_B^N = 0.4$ *and* $\Pi = 8.$ *and different values of* H_L/H_S*. Squares, circles and triangles stand for* H_L/H_S=[2, 8, 16]*, while empty and filled symbols represent results for the nozle (N) and diffusor (D) directions, respectively.*

Finally, Figure 2 shows the distribution of the pressure and the rarefaction parameter as a function of the aspect ratio H_L/H_S for $\delta_B^N = 0.4$ and $\Pi = 8.$ The deviation of these profiles from the typical curves for uniform channels is more stronger if the aspect ratio is larger, i.e. the channel is more tapered.

5. Conclusions

In this paper, the kinetic calculation of isothermal pressure driven single gas flows in long tapered rectangular channels is presented and the corresponding results are shown. The solution of the problem is divided into two stages. First the local flow problem is defined on the kinetic level. The linearized BGK kinetic equation is used to model the flow and solved by standard and accelerated discrete velocity methods in a wide range of gaseous rarefaction and at numerous values of the aspect ratio of the cross section. The calculated dimensionless flow rates form a database. Secondly, the mass flow rate and the distribution of the pressure and the rarefaction parameter are determined on the basis of the conservation of mass. Results in terms of the flow rate are delivered for a test tapered channel in the whole range of gaseous rarefaction. It is shown that at the same inlet and outlet pressures, the flow rate is larger in the nozle than diffusor direction. This diodicity effect has a maximum in the transition region. Results for the axial

distribution of the pressure and the rarefaction parameter are also shown. The profiles are quite different to those for uniform capillaries. In the present case, the pressure exhibits a sharp change near the small cross section, and the rarefaction parameter for the diffusor case increases along the axis of the channel even if the pressure is decreasing. The diodicity effect can be useful in constructing micropumps. It is shown that maximal diodicity can be reached in the transition region. Hence, the corresponding devices should operate in this rarefaction range.

Acknowledgment

This research obtained financial support from the Marie Curie Action COFUND of the European Community's Seventh Framework Programme for Research and Technological Development (2007-2013) in the Project Bremen TRAC.

References

1. Kandlikar, S.G., Garimella, S., et al., 2006. Heat transfer and fluid flow in minichannels and microchannels. Elsevier, Oxford.
2. Li, D. (Ed.), 2008. Encyclopedia of Microfluidics and Nanofluidics. Springer-Verlag.
3. Cercignani, C., 2006. Slow Rarefied flows: Theory and Applications to Micro-electro-mechanical systems. Birkhauser Verlag.
4. Sharipov, F., 1999. Rarefied gas flow through a long rectangular channel. J. Vac. Sci. Technol. A 17, 3062-3066.
5. Sharipov, F., Seleznev, V., 1994. Rarefied flow through a long tube at any pressure ratio. J. Vac. Sci. Technol. A 12, 2933-2935.
6. Szalmas, L., 2013. Accelerated discrete velocity method for axial-symmetric gaseous flows. Comput. Phys. Commun. 184, 1432-1438.
7. Graur, I., Sharipov, F., 2007. Gas flow through an elliptical tube over the whole range of the gas rarefaction. Eur. J. Mech. B/Fluids 27, 335-345.
8. Naris, S., Valougeorgis, D., 2008. Rarefied gas flow in a triangular duct based on a boundary fitted lattice. Eur. J. Mech. B/Fluids 27, 810-822.
9. Szalmas, L., Valougeorgis, D., 2010. A fast iterative model for discrete velocity calculations on triangular grids. J. Comput. Phys. 229, 4315-4326.
10. Varoutis, S., Naris, S., Hauer, V., Day, C., Valougeorgis, D., 2009. Computational and experimental study of gas flows through long channels of various cross sections in the whole range of the Knudsen number. J. Vac. Sci. Technol. A 27, 89-100.
11. Bird, G.A., 1994. Molecular gas dynamics and the direct simulation of gas flows. Oxford, University Press.
12. Radtke, G.A, Hadjiconstantinou, N.G., 2009. Variance-reduced particle simulation of the Boltzmann transport equation in the relaxation-time approximation. Phys. Rev. 79, 056711.
13. Szalmas, L., 2012. Variance-reduced DSMC for binary gas flows as defined by the McCormack kinetic model. J. Comput. Phys. 231, 3723–38.
14. Szalmas, L., 2013. Varience-reduced DSMC method for axial-symmetric flows of gaseous mixtures. Comput. Fluids 74, 58-65.
15. Szalmas, L., 2013. Flows of rarefied gaseous mixtures in networks of long channels. Microfluid. Nanofluid. 15, 817-827.